A Multiregion Assessment of Observed Changes in the Areal Extent of Temperature and Precipitation Extremes

ANDREA J. DITTUS AND DAVID J. KAROLY

School of Earth Sciences, and Australian Research Council Centre of Excellence for Climate System Science, University of Melbourne, Parkville, Victoria

SOPHIE C. LEWIS

Research School of Earth Sciences, and Australian Research Council Centre of Excellence for Climate System Science, Australian National University, Canberra, Australian Capital Territory

LISA V. ALEXANDER

Climate Change Research Centre, and Australian Research Council Centre of Excellence for Climate System Science, University of New South Wales, Sydney, New South Wales, Australia

ABSTRACT

This study examines trends in the area affected by temperature and precipitation extremes across five large-scale regions using the climate extremes index (CEI) framework. Analyzing changes in temperature and precipitation extremes in terms of areal fraction provides information from a different perspective and can be useful for climate monitoring. Trends in five temperature and precipitation components are analyzed, calculated using a new method based on standard extreme indices. These indices, derived from daily meteorological station data, are obtained from two global land-based gridded extreme indices datasets. The four continental-scale regions of Europe, North America, Asia, and Australia are analyzed over the period from 1951 to 2010, where sufficient data coverage is available. These components are also computed for the entire Northern Hemisphere, providing the first CEI results at the hemispheric scale. Results show statistically significant increases in the percentage area experiencing much-above-average warm days and nights and much-below-average cool days and nights for all regions, with the exception of North America for maximum temperature extremes. Increases in the area affected by precipitation extremes are also found for the Northern Hemisphere regions, particularly Europe and North America.

1. Introduction

''Climate extreme'' is a broad term covering many different types and aspects of extremes, including high-impact events, such as heat waves and floods and more moderate extremes, such as warm days and nights or very wet days. The definitions of extreme vary depending on the application. Data availability is one of the main limitations to analyzing past changes in extremes, and this is particularly the case for very rare events.

To try to address these limitations, the joint World Meteorological Organization (WMO) Commission for Climatology (CCl)/World Climate Research Programme (WRCP)/Joint WMO–Intergovernmental Oceanographic Commission (IOC) Technical Commission for Oceanography and Marine Meteorology (JCOMM) Expert Team on Climate Change Detection and Indices (ETCCDI) created a suite of 27 recommended ''extreme indices'' in an effort to standardize the indices used internationally and to encourage the exchange of data in regions where data policies on the use of raw data were restrictive or complicated. This allowed comparisons between different regions and different studies, particularly encouraging analysis of climate extremes in regions of the world where data were sparse or not publicly available (Zhang et al. 2011). Datasets of global climate extremes indices

Corresponding author address: Andrea J. Dittus, School of Earth Sciences, University of Melbourne, Melbourne VIC 3010, Australia.
E-mail: adittus@student.unimelb.edu.au

(HadEX; Alexander et al. 2006) and HadEX2 (Donat et al. 2013b) are datasets that resulted from this coordinated effort. Studies such as Alexander et al. (2006) and Donat et al. (2013b) have documented global increases in warm temperature extremes and decreases in cold temperature extremes. There have also been increases in heavy precipitation events in some regions, although these have been more spatially heterogeneous (e.g., Seneviratne et al. 2012; Donat et al. 2013b; Alexander et al. 2006; Groisman et al. 2005).

As a tool to further understand complex multivariate information, Karl et al. (1996) proposed an approach combining different types of extremes for the United States. The climate extremes index (CEI) consists of monthly mean temperature, drought, and daily precipitation extremes indicators based on the percentage area affected by extreme conditions. The CEI framework allows comparison of different types of extremes on an equal basis, as the components for the different extremes are expressed in the same percentage area units and have the same expected values. It can thus provide a concise overview of temperature and precipitation extremes occurring in a region, and identify potential interactions between these. Extreme conditions, or much-above (below)-average conditions correspond to conditions falling in the lower and upper 10th percentile of the distribution. For the drought and heavy precipitation indicators, absolute thresholds were used in Karl et al. (1996). A revised CEI by Gleason et al. (2008) introduced definitions based on the lower and upper 10th percentile for these indicators as well. Percentile thresholds ensure that the CEI can be calculated anywhere, as they are calculated for each location.

In both these CEIs (Karl et al. 1996; Gleason et al. 2008), upper- and lower-tail extremes are added and the expected percentage area experiencing extreme conditions would therefore be 20%. However, this approach does not distinguish between changes in the occurrence of extremes in the upper and lower tails of the distribution. Therefore, in a situation where the trends in one tail are increasing and decreasing in the other (e.g., as a result of a simple shift in the distribution), trends in one tail could partly offset trends in the other tail, creating difficulties for interpretation of long-term changes. Gallant and Karoly (2010) therefore introduced a variant of the CEI, the modified CEI (mCEI), where extremes in one tail are subtracted from extremes in the other tail, instead of adding them. This ensures that directional information is included in the CEI and its components, and that changes in both tails can be identified. Warm extremes have typically been combined with wet extremes and cool extremes with dry extremes. This combination is appropriate to highlight the long-term trends over large areas, as for many regions apart from the subtropics, increasing trends are expected for both warm and wet extremes.

As daily events often have large socioeconomic impacts, Gallant and Karoly (2010) further introduced the daily modified CEI (dmCEI), using daily temperature extremes rather than monthly and annual average temperature extremes (Gallant and Karoly 2010, and references therein). The mCEI has been calculated for three regions to date: the United States, Europe and Australia, while the dmCEI has only been calculated for Europe and Australia, because of a lack of suitable daily temperature data for the United States (Gallant et al. 2014, hereinafter GKG2014). Data availability, quality, and accessibility are the major factors that limit the applicability of the dmCEI to other regions.

To address these limitations, this study introduces a new CEI variant: the ETCCDI-based modified CEI (EmCEI). The EmCEI is calculated from the standard, readily available extreme indices described above. The indices are computed from daily data, therefore containing information regarding daily extremes. The EmCEI therefore resembles the dmCEI but since we are using extreme indices as input, data availability is increased while computational demands are significantly reduced. As some precipitation ETCCDI indices are only available annually, we present only annual EmCEI results in this paper. To obtain maximal coverage two extreme indices datasets, the Global Historical Climatology Network–Daily (GHCND)-based gridded temperature and precipitation climate extremes indices (GHCNDEX; Donat et al. 2013a) and HadEX2 (Donat et al. 2013b), are used in this study. The GHCNDEX indices are updated operationally by the NOAA/National Centers for Environmental Information (NCEI) at the station level and gridded by researchers at the University of New South Wales, Australia. This allows the EmCEI to be routinely updated for regions with sufficient data coverage. GHCNDEX and HadEX2 are publicly available online (at www.climdex.org). The EmCEI is calculated for Europe, North America, Asia, Australia, and the Northern Hemisphere. For the first time, a CEI is presented at the hemispheric scale. This new method provides an efficient tool to document and investigate large-scale changes in temperature and precipitation extremes over different regions. In particular, it allows the identification of which aspects of these extremes are increasing, decreasing, or unchanged over a region. Using the same metric across regions and across components, it thus provides an overview of the long-term trends in various aspects of temperature and precipitation extremes in different regions.

This paper is structured as follows. Section 2 introduces the different components of the EmCEI, how they are calculated, and the data used to compute them.

TABLE 1. Indices used to calculate the EmCEI and its components. The top seven indices are the ETCCDI indices used (Zhang et al. 2011). The bottom four modified indices with asterisks are used in the calculation of the EmCEI and its components. The subscripts y is for the yearly value and mean is for the mean over all years, and σ(PRCPTOT) denotes standard deviation of PRCPTOT.

Index	Description	Definition
TN10p (%)	Cool nights	Percentage of time when daily min temperature <10th percentile
TX10p (%)	Cool days	Percentage of time when daily max temperature <10th percentile
TN90p (%)	Warm nights	Percentage of time when daily min temperature >90th percentile
TX90p (%)	Warm days	Percentage of time when daily max temperature >90th percentile
SDII (mm day^{-1})	Simple daily intensity index	The ratio of annual total precipitation to the number of wet days (>1 mm)
R95p (mm)	Very wet days	Annual total precipitation from days >95th percentile
PRCPTOT (mm)	Annual total wet-day precipitation	Annual total precipitation from days ≥1 mm
Index	Formula	Definition
R95PTOT*	R95p/PRCPTOT	Annual contribution of very wet days to total precipitation
SP*	(PRCPTOT$_y$ − PRCPTOT$_{mean}$)/σ(PRCPTOT)	Annual standardized precipitation anomaly
WD*	PRCPTOT/SDII	Annual number of wet days
DD*	365 − WD*	Annual number of dry days

Section 3 presents the results for the four continental-scale regions mentioned above and the Northern Hemisphere. A comparison with GKG2014 is also performed for Europe and Australia. Further, the utility and limitations of combining the components to form the combined EmCEI index are discussed. The relationship and significance of the EmCEI results in relation to changes in mean temperature and total precipitation are discussed in section 4. Finally, the conclusions of this paper are presented in section 5.

2. Methods and data

a. Definition of components

Like the original CEI (Karl et al. 1996) and its modifications (e.g., Gallant and Karoly 2010; GKG2014), the EmCEI consists of five temperature and precipitation components. The average of these components corresponds to the EmCEI and is discussed in section 3f. These components include a maximum and a minimum temperature component, a total rainfall, a heavy rainfall, and a wet-day/dry-day component. The total rainfall component replaces the Palmer drought severity index (PDSI) component previously used in CEI studies. The PDSI is sensitive to the method used to calculate evapotranspiration (Sheffield et al. 2012), which makes the total precipitation component a simpler, less problematic alternative that can be used for any region.

Each component measures the percentage of an area with much above or below average conditions in the

variable considered. The five components are calculated using seven climate extremes indices (four temperature indices and three precipitation indices) from the so-called ETCCDI indices, hence its name "ETCCDI-based modified climate extremes index." The seven ETCCDI indices used are (for more details see Table 1):

- warm and cool days (TX90p and TX10p, respectively), which are based on daily maximum temperature and represent the annual percentage of days where the maximum temperature is above the 90th or below the 10th percentile;
- warm and cool nights (TN90p and TN10p, respectively), which are based on daily minimum temperature and follow the same definitions as their maximum temperature equivalent;
- total annual precipitation on days where precipitation is equal to or exceeds 1 mm (PRCPTOT);
- precipitation amount from heavy rain days (R95p), which corresponds to the total amount of rainfall per year that fell on days where the 95th percentile was exceeded, that is, the precipitation amount from heavy rain days; and
- simple daily intensity index (SDII), which corresponds to the average daily precipitation on a wet day (millimeters per day).

The SDII and PRCPTOT are used to calculate the number of wet and dry days used in component 5 (C5; see Table 2). SDII corresponds to the average daily

TABLE 2. EmCEI component definitions. The percentile thresholds are calculated using all years for the time period considered. The definition of the indices used to calculate the components defined here can be found in Table 1.

Component	Definition
Max temp (C1)	Percentage area where warm days exceed the 90th percentile minus percentage area where cool days exceed the 90th percentile.
Min temp (C2)	Percentage area where warm nights exceed the 90th percentile minus percentage area where cool nights exceed the 90th percentile.
Total rainfall (C3)	Percentage area where the standardized annual precipitation anomaly exceeds the 90th percentile minus percentage area where it is less than the 10th percentile.
Heavy rainfall (C4)	Percentage area where the contribution from heavy rainfall to total rainfall exceeds the 90th percentile minus percentage area where the contribution from heavy rainfall to total rainfall is below the 10th percentile.
Wet and dry days (C5)	Percentage area where the number of wet days exceeds the 90th percentile minus percentage area where the number of dry days exceeds the 90th percentile.

precipitation on a wet day (millimeters per day). Therefore, we can calculate the total number of wet days by dividing the total annual precipitation amount with SDII. Using the number of wet days, the total number of dry days is calculated as the remaining number of days per year, using 365 days in a year. Please note that the calculation of the ETCCDI indices allows up to 15 missing days per year before the index is set to missing. Therefore, any missing data will be implicitly counted as a dry day.

Each component of the EmCEI consists of two parts, corresponding to the upper and lower-tail extremes (Table 2):

1) The maximum temperature component corresponds to the percentage area where the frequency of warm days (TX90p) is above the long-term 90th percentile minus the percentage area where the frequency of cool days (TX10p) is above the long-term 90th percentile.
2) The same definition is applied for the minimum temperature component using warm (TN90p) and cool nights (TN10p).
3) The total precipitation component measures the area where a standardized annual precipitation anomaly (SP*, derived from PRCPTOT; see Table 1) exceeds the 90th percentile minus the percentage area where it is less than the 10th percentile.
4) The heavy rainfall component measures the percentage area where the proportion of annual rainfall due to heavy rain days (R95pTOT*; see Table 1) exceeds the 90th percentile minus the percentage area where it is less than the 10th percentile.
5) The wet- and dry-day component measures the percentage area where the number of wet days (WD*; see Table 1) exceeds the 90th percentile minus the percentage area where the number of dry days (DD*; see Table 1) exceeds the 90th percentile.

The definition of component 4 is different from GKG2014, where component 4 is based on the upper tail only and subsequently doubled with the mean removed. The percentile thresholds are calculated at each grid point using all data available over the entire period from 1951 to 2010. For every year at every grid point, the data value is checked to see whether it exceeds the percentile threshold for that grid box. If it does, then the area of this grid box is counted toward the percentage area experiencing extreme conditions in that year. To show the respective contribution of each tail to each component, both the upper and lower tail is shown for the annual values. However, for the long-term trend analysis (including the 5-yr running mean shown in Figs. 2–7) and the calculation of all the correlation coefficients (see Tables 4 and 5), the components defined as the difference between the upper and lower tail (as described above) are used. The EmCEI components and subcomponents are made available online (at https://researchdata.ands.org.au/time-series-emcei-components-subcomponents/512056).

b. Data and quality control

In this study two extreme indices datasets are used for the calculation of the EmCEI and its components. HadEX2 (Donat et al. 2013b) is an extreme indices dataset covering the period 1901–2010, while GHCNDEX (Donat et al. 2013a) is an operational extreme indices dataset, starting in 1951. Most importantly, they have different data sources and different quality control procedures, which result in two datasets with different spatial resolutions and different temporal and spatial coverage. HadEX2 contains mostly quality controlled data from researchers in the country of origin, along with data from targeted regional workshops. GHCNDEX is sourced from the Global Historical Climatology Network–Daily (Menne et al. 2012) but only uses stations that have at least 40 years of data. The resolution of HadEX2 is 3.75° longitude × 2.5° latitude and that of GHCNDEX is 2.5° longitude × 2.5° latitude. GHCNDEX has better coverage over Australia for the precipitation indices as only high-quality data sourced from the Australian Bureau of
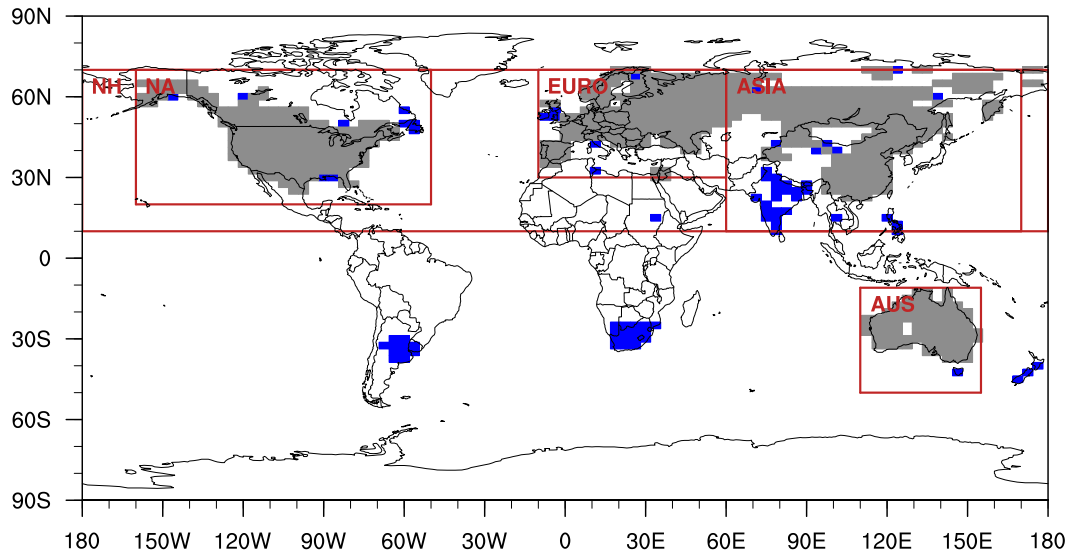
FIG. 1. Geographical coverage for 1951–2010 for the heavy rainfall (R95p) index is shown. The gray boxes indicate data originating from GHCNDEX; the blue boxes indicate data from HadEX2. Only grid boxes where at least 80% of data over all years and 80% in the first and last 10 years were available are used in this study and shown here. As heavy rainfall has the lowest coverage, all other indices were masked to the coverage shown here.

Meteorology are used in HadEX2. We have used the version of HadEX2 created on 9 February 2015 and the GHCNDEX version from 10 February 2015.

To obtain the best possible coverage, a merged dataset was created using HadEX2 and GHCNDEX. While there are many potential issues associated with merging two datasets, we assess that this will have little effect on our results, since the value at each grid box is assessed against a threshold calculated from that grid box's corresponding dataset. GHCNDEX was regridded to the resolution of HadEX2 using a first-order conservative remapping procedure (Jones 1999). As both datasets have time-varying spatial coverage for all indices, only the grid boxes where at least 80% of all years and 80% of years in the first and last 10 years contained complete data were kept for each index. This was done to ensure continuity of record at each grid box and resulted in a nearly time invariant coverage mask for each index. HadEX2 grid boxes were added where GHCNDEX contained missing data over the entire period. Finally, the spatial coverage for all indices was masked with the R95p data coverage, as the spatial coverage for this index in the Northern Hemisphere is much lower than the other indices, particularly the temperature indices. The resulting global coverage is shown in Fig. 1. Four continental-scale and one hemispheric-scale regions are analyzed: North America, Europe, Asia, Australia, and the Northern Hemisphere from 20° to 70°N (Table 3).

Prior to trend estimation and significance testing, the data were prewhitened following Wang and Swail (2001) to account for autocorrelation in the time series (see also Zhang and Zwiers 2004; Zhang et al. 2000), which when present is known to artificially inflate the statistical significance of a trend. This is an iterative procedure where the lag-1 autocorrelation is repeatedly estimated and removed from the original time series. The slope of the time series is then estimated from the prewhitened time series, and the trend is then removed from the original time series using this estimate. We have used the R package zyp (Bronaugh and Werner 2013) for this purpose. The trends were calculated using the nonparametric Theil–Sen slope estimator (Sen 1968). Statistical significance was assessed at the 5% level throughout using the nonparametric Mann–Kendall trend test (Kendall 1975).

In section 4, the relationship of the EmCEI components to mean changes in temperature and precipitation are discussed. The data for mean temperature anomalies and total precipitation used are from the Climate Research Unit and Hadley Centre temperature anomalies, version 4 (CRUTEM4; Jones et al. 2012), and the GPCC full data reanalysis, version 6.0 (Schneider et al. 2011, 2014; Becker et al. 2013), datasets, respectively. The GPCC data were regridded to HadEX2 resolution using a first-order conservative remapping procedure and masked to the coverage shown in Fig. 1. In the case

TABLE 3. Definition of the regions used in this study.

Region	Min lat	Max lat	Min lon	Max lon
Europe	30°N	70°N	10°W	60°E
NA	20°N	70°N	160°W	50°W
Asia	10°N	70°N	60°E	170°E
Australia	50°S	11°S	110°E	155°E
NH	10°N	70°N	All longitudes	

EURO Maximum temperature

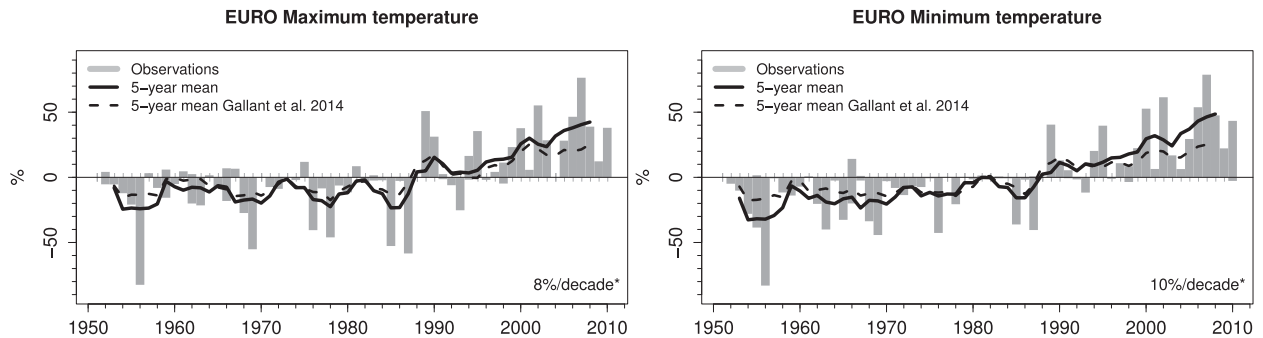**EURO Minimum temperature**

FIG. 2. Maximum and minimum temperature components of the EmCEI for Europe. These components represent the percentage area of the European region that is experiencing a much-above-average frequency of warm days or warm nights (positive values) and the percentage area experiencing much-above-average frequency of cool days or cool nights (negative values). The solid black line corresponds to the 5-yr running mean of the temperature components where the lower-tail extremes have been subtracted from the upper-tail extremes. For exact definitions please see Table 2. Trends (% decade^{-1}) were calculated using the nonparametric Theil–Sen slope estimator. An asterisk indicates statistical significance at the 5% level using the Mann–Kendall trend test.

of CRUTEM4, the coverage mask shown in Fig. 1 was regridded to the resolution of CRUTEM4, as its resolution is lower than that of HadEX2. An area average of annual means was subsequently computed and the data detrended using the Theil–Sen slope estimator.

3. Regional results

Results for the EmCEI components are presented for Europe, North America, Asia, Australia, and the entire Northern Hemisphere. The relationships between components and the utility of a combined index are then discussed for all regions. Data availability was not sufficient to calculate a Southern Hemisphere EmCEI.

a. Europe

Over Europe, strong and statistically significant trends in the maximum and minimum temperature components of 8% and 10% decade^{-1}, respectively, are found (Fig. 2). As in GKG2014, the trend in the minimum component is larger than for maximum temperature. These trends document an increase in the percentage of area in Europe that is experiencing much-above-average warm days and nights and a decrease in the percentage of Europe experiencing much-above-average cool days and nights.

The total precipitation component shows a statistically significant increase of 4% decade^{-1} in the percentage of Europe that experiences much-above-average annual precipitation (Fig. 3). The percentage area experiencing a much-above-average contribution of heavy rainfall and the percentage area with much above average number of wet days have also increased, by 3% and 2% decade^{-1}, respectively (statistically significant). Note that in Fig. 3 for the precipitation components, many years have both

much-above-normal and much-below-normal contributions. However, for the temperature components in Fig. 2, most years have a contribution from either much above or much below normal, but not both. This is because the spatial coherence of temperature extremes is much larger than for precipitation extremes.

There is good agreement with results from GKG2014 for the temperature components, the wet- and dry-day components, and the combined index, with correlation coefficients between the EmCEI and GKG2014 components exceeding 0.8 for all of these components (Table 4). The total and heavy precipitation components, however, are substantially different between the two methods, the EmCEI components showing larger increases in the area with much-above-average total rainfall and the contribution from heavy rainfall than GKG2014. This could be due to differences between the datasets as well as a sensitivity of the precipitation components to data resolution, as the input data for the EmCEI is much coarser than the data used in GKG2014. Given the high spatial variability of precipitation events, it is likely that resolution and data source could have a large effect on the precipitation components. Additionally, the change from a Palmer drought severity index–based component 3 to a standardized precipitation anomaly might also have contributed to the difference between those components.

Our findings are consistent with increases in warm temperature extremes and decreases in cold temperature extremes over Europe found in other studies (e.g., Klein Tank and Können 2003; Donat et al. 2013b). Studies of precipitation extremes over Europe have shown that increases are strongest in the cold season (e.g., Moberg et al. 2006). It is thus likely that the observed increase in areal extent of wet extremes is primarily due to increases occurring in cold months.
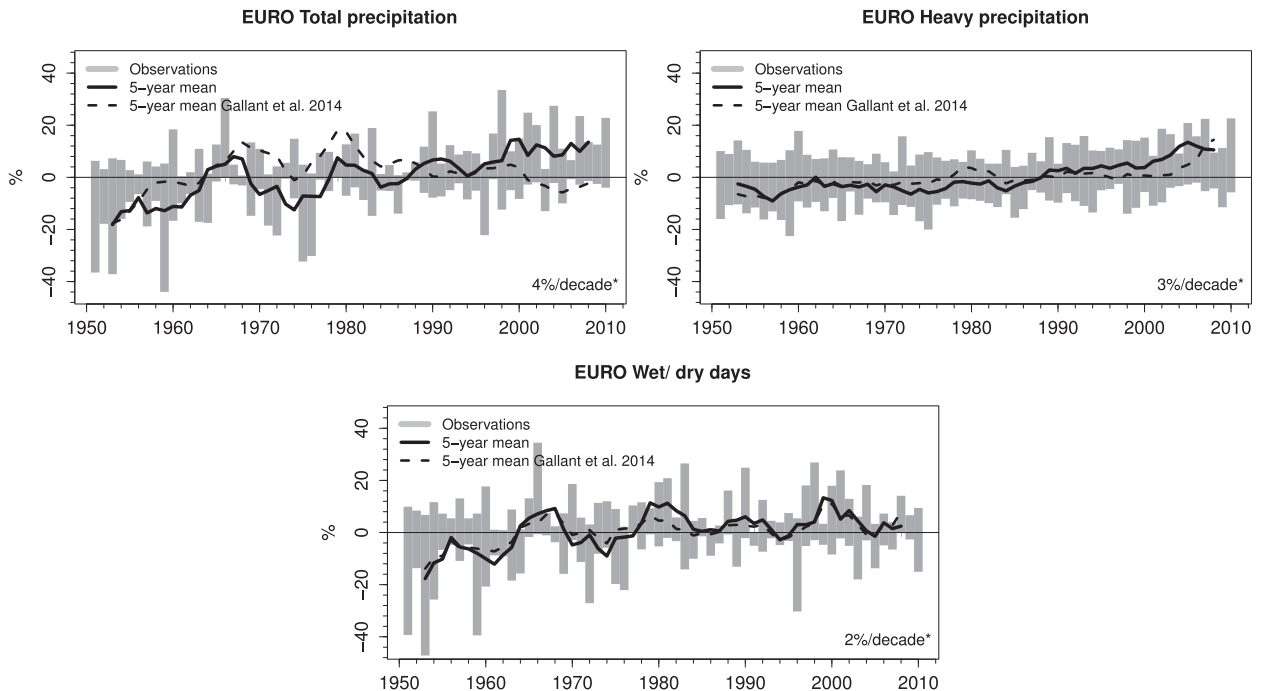
FIG. 3. The precipitation components of the European EmCEI are shown. The gray bars show the percentage area experiencing wet extremes (positive values) and the percentage area experiencing dry extremes (negative values). The solid black line corresponds to the running mean of each of the components where the lower-tail extremes have been subtracted from the upper-tail extremes. For the total precipitation component, positive values represent the percentage area where annual total rainfall is much above average and the negative values the percentage area where the total annual rainfall is much below average. Similarly, the heavy rainfall component corresponds to the percentage area where the contribution from heavy precipitation to total precipitation is much above average and the percentage area where the contribution from heavy precipitation to total precipitation is much below average. Finally, the wet and dry components correspond to the percentage area with much-above-normal number of wet days and the percentage area with much-above-average number of dry days. Trends (% decade^{-1}) were calculated using the nonparametric Theil–Sen slope estimator. An asterisk indicates statistical significance at the 5% level using the Mann–Kendall trend test.

b. North America

To date there is no CEI available based on daily temperature data for the United States. As such, the EmCEI presented here for the North American region is the first CEI variant to include daily temperature extremes. The trend in the maximum temperature component of the EmCEI is weak (1% decade^{-1}, not statistically significant); this component appears to be dominated by interannual to decadal variability (Fig. 4). This is in contrast to the mCEI (GKG2014), which shows a significant increase of approximately 5% decade^{-1}. Here, the areal extent of cold extremes is increasing until the 1970s and a greater extent of cold extremes relative to warm extremes remains relatively frequent until the last decade. The differences to the mCEI are likely primarily due to the inclusion of daily extremes in the EmCEI. Another difference between the mCEI and EmCEI consists of the larger area represented in the EmCEI (including parts of Canada and Alaska).

The minimum temperature component shows large increases (6% decade^{-1}, statistically significant) in the area experiencing more frequent warm nights and decreases in the area with above-average cold nights, consistent with the findings of GKG2014. Statistically significant increases are found in the areal extent of all precipitation-related components. The total rainfall and wet and dry days are again very similar, with large decadal variability. An increase in the area experiencing much-above-normal annual rainfall (4% decade^{-1}) is observed. The trends in the heavy rainfall and wet- and dry-day components are of the same magnitude (3% decade^{-1} for both components) and indicate an increase in the area both experiencing much-above-average

TABLE 4. Spearman correlation coefficient between the GKG2014 and EmCEI components 1–5 for Australia and Europe.

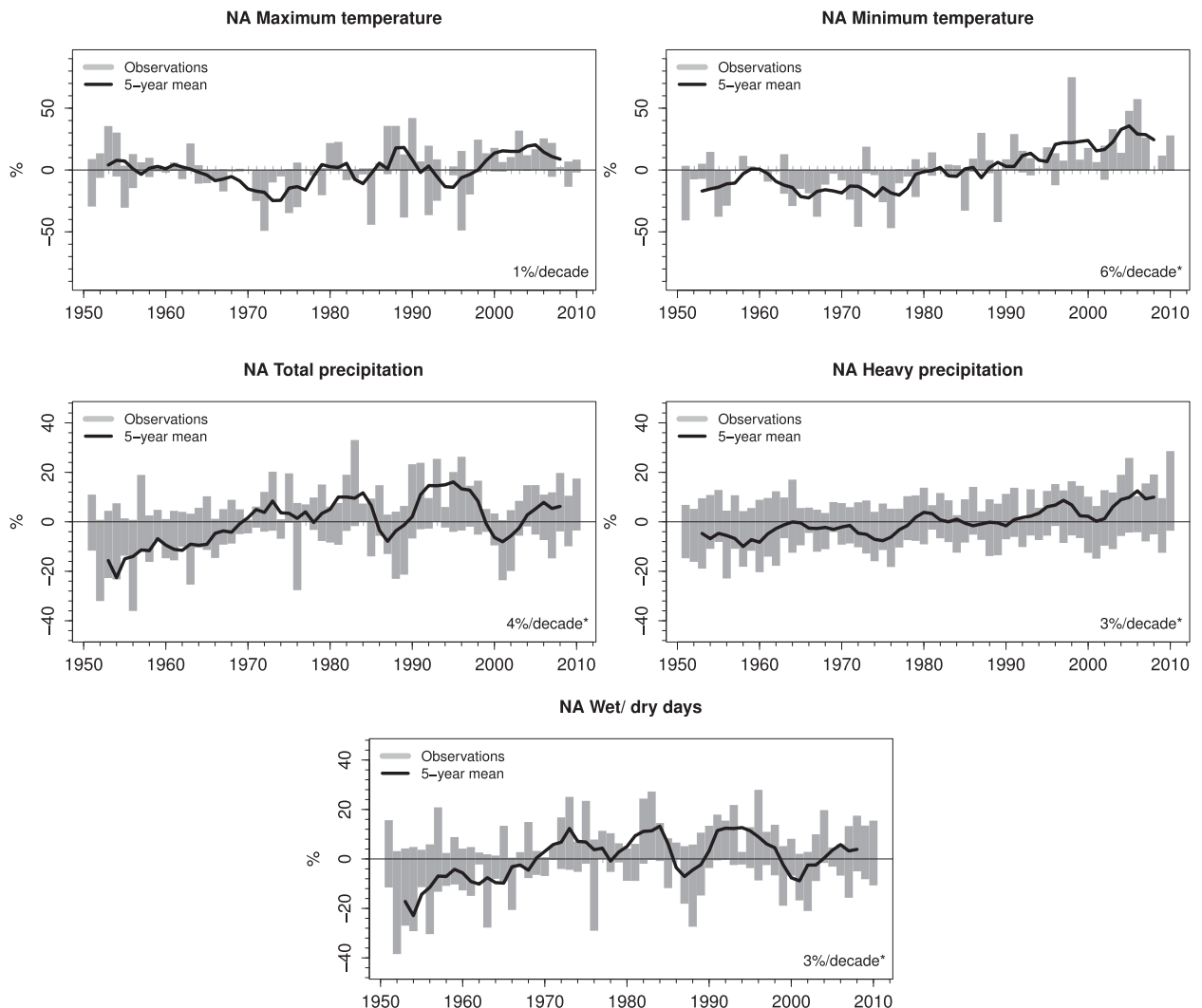| Region	C1	C2	C3	C4	C5	EmCEI/dmCEI
Europe	0.87	0.86	0.44	0.65	0.84	0.89
Australia	0.81	0.93	0.61	0.61	0.92	0.93

FIG. 4. EmCEI components for North America. Please refer to Table 3 and Fig. 1 for the definition and coverage of the North American region. Trends (% decade^{-1}) were calculated using the nonparametric Theil–Sen slope estimator. An asterisk indicates statistical significance at the 5% level using the Mann–Kendall trend test.

heavy rainfall and wet days. Despite using different data and spatial resolution (1° longitude × 1° latitude for daily precipitation over the United States in GKG2014), the EmCEI rainfall components show similar temporal variations to the mCEI of GKG2014.

c. Asia

The Asian EmCEI presented here is the first combined climate extremes index for this region, with the exception of a three-component CEI (CEI-3) for the Russian Federation by Gruza et al. (1999). Large increases in the maximum and minimum temperature components are observed, the minimum temperature component trend being substantially larger than the maximum temperature increase, reaching 11% decade^{-1} (Fig. 5). This is a larger trend than observed for any

other region and shows that the area of Asia experiencing much-above-average warm nights has rapidly increased. The area experiencing rainfall extremes has increased at a more moderate pace, with much of the observed increase in area experiencing above-normal total rainfall and heavy rainfall occurring in the second half of the 60-yr period examined. The trends in the area experiencing much-above-average total precipitation and a much-above-average proportion of heavy precipitation are small but statistically significant (2% and 1% decade^{-1}, respectively). There does not appear to be a trend in the area with above-average numbers of wet and dry days (Fig. 5).

Our results are consistent with the findings of other studies, such as Klein Tank et al. (2006), Zhou and Ren (2011), and You et al. (2011), who found stronger trends
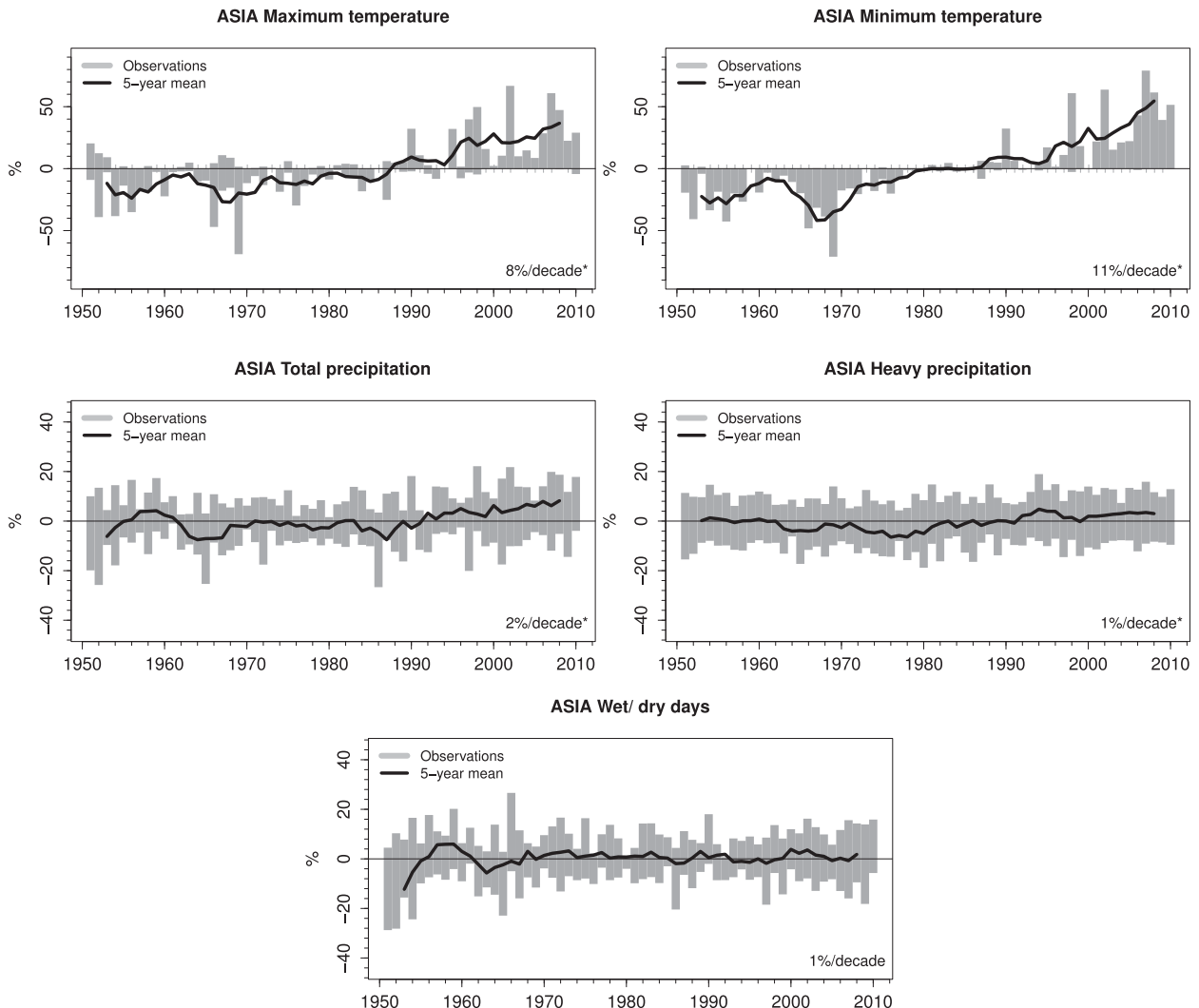
FIG. 5. EmCEI components for Asia. Please refer to Table 3 and Fig. 1 for the definition and coverage of the Asian region. Trends (% decade^{-1}) were calculated using the nonparametric Theil–Sen slope estimator. An asterisk indicates statistical significance at the 5% level using the Mann–Kendall trend test.

in minimum temperature extremes than maximum temperature extremes. Klein Tank et al. (2006) suggest the trends in maximum temperature extremes in the second half of the century are part of multidecadal variability, resulting from finding trends of opposite sign in the first half of the century. With regard to precipitation extremes, Klein Tank et al. (2006) and You et al. (2011) found statistically significant increases in very wet day precipitation (above the 95th percentile) and in the contribution from very wet days to total precipitation (Klein Tank et al. 2006), which is consistent with our results.

d. Australia

The maximum and minimum temperature components for Australia exhibit strong increasing trends,

exceeding 7% and 8% decade^{-1}, respectively. This reflects an increase in the area with much-above-average frequency of warm days and nights and a decrease in the area with much-above-average cool days and nights (Fig. 6).

None of the precipitation components shows statistically significant trends. The total rainfall and wet- and dry-day components (Fig. 6) show small, not statistically significant increasing trends (3% decade^{-1} in both cases), while there is no evidence of any trend in the heavy rainfall component. The total rainfall and wet- and dry-day components are very similar, indicating that annual total rainfall is closely related to the number of wet days; that is, areas that receive much-above-average annual rainfall also experienced much-above-average number of wet days. It suggests that the number of wet days is
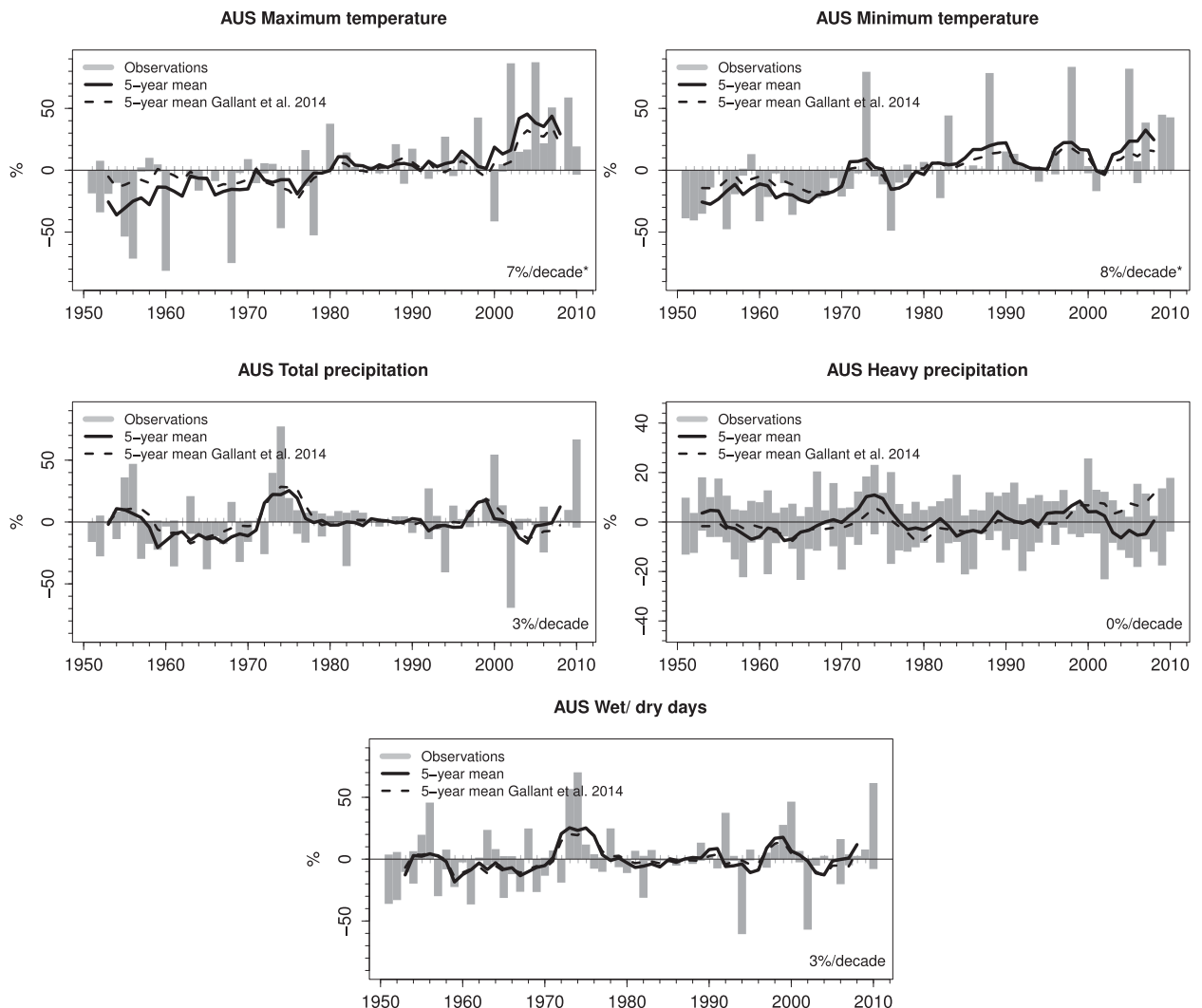
FIG. 6. EmCEI components for Australia. Please refer to Table 3 and Fig. 1 for the definition and coverage of the Australian region. Trends (% decade^{-1}) were calculated using the nonparametric Theil–Sen slope estimator. An asterisk indicates statistical significance at the 5% level using the Mann–Kendall trend test.

more important for determining the amount of annual rainfall than for heavy rainfall events. For the rainfall components, decadal variability appears to be dominant. This is particularly apparent as several periods where large areas received much-above-average total rainfall and had much-above-average number of wet days, for example, several years in the 1970s. These periods coincide with La Niña years, suggesting that El Niño–Southern Oscillation (ENSO) is playing an important role in driving the decadal variability in these components. It is well known that Australia's rainfall is more variable than similar climates elsewhere in the world (Nicholls et al. 1997) and a large part of this variability is associated with ENSO (e.g., Risbey et al. 2009; Nicholls et al. 1997). Australia is the only region for

which the areal extent of rainfall extremes (components 3 and 5) reaches comparable magnitudes to the temperature components at the interannual scale (from approximately −70% to +80%). The large spatial extent of the rainfall extremes observed in this region is likely due to the influence of ENSO on rainfall across much of the Australian continent.

The correlation coefficients between the EmCEI components and GKG2014 components show good agreement between the two methods, particularly for the temperature components (Table 4). The lowest correlation coefficients are found for the total precipitation and heavy precipitation components (0.61 for both). This is not surprising, as these are the components that are defined differently than in GKG2014.
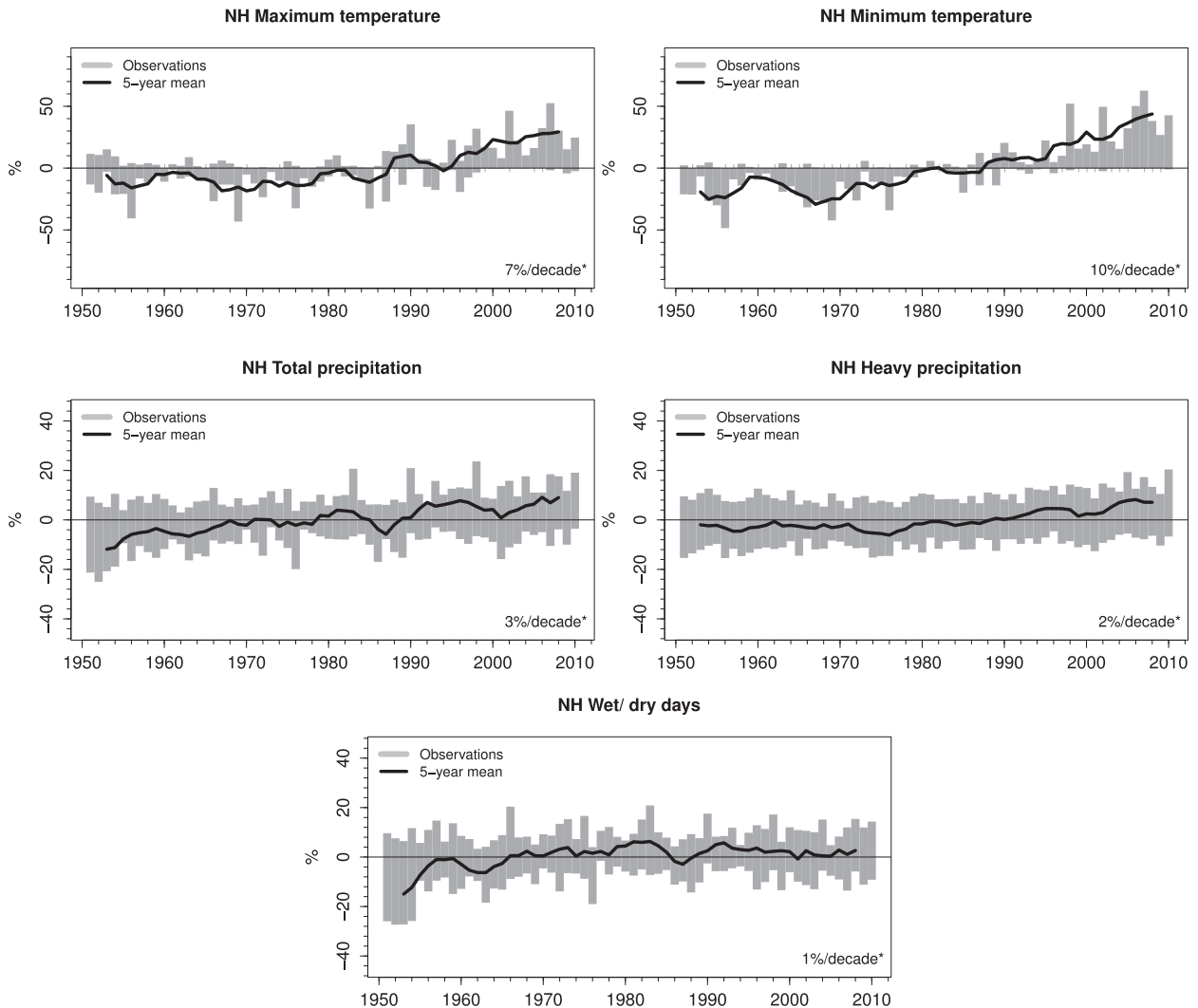
FIG. 7. The EmCEI components are shown for the Northern Hemisphere. Trends (% decade^{-1}) were calculated using the nonparametric Theil–Sen slope estimator. An asterisk indicates statistical significance at the 5% level using the Mann–Kendall trend test.

e. Northern Hemisphere

For the first time, a climate extremes index is computed at the hemispheric scale. The Northern Hemisphere region spans the continental-scale regions of Europe, North America, and Asia as discussed above (Fig. 1). Over the Northern Hemisphere, warm maximum and minimum temperature extremes have become increasingly widespread throughout the period from 1951 to 2010 (Fig. 7). Concurrently, the spatial extent of cold maximum and minimum temperature extremes has decreased. The late 1960s were a period during which large areas of the Northern Hemisphere were experiencing cold nights much more frequently than usual, particularly in Asia (Fig. 5). The minimum temperature trend is stronger than

for maximum temperature, with a 10% increase per decade in this component. GKG2014 also found that the spatial extent of minimum temperature extremes increased faster than maximum temperature for the United States (mCEI) and Europe (mCEI and dmCEI). This is consistent with other studies, such as Donat et al. (2013b), who found that temperature extremes derived from daily minimum temperatures have warmed faster than extremes derived from daily maximum temperature. The trends for both maximum and minimum temperatures are highly statistically significant.

Increasing trends are also observed for the precipitation components, in particular the total precipitation component; all three are statistically significant (3%, 2%, and 1% decade^{-1}, respectively). This reflects a
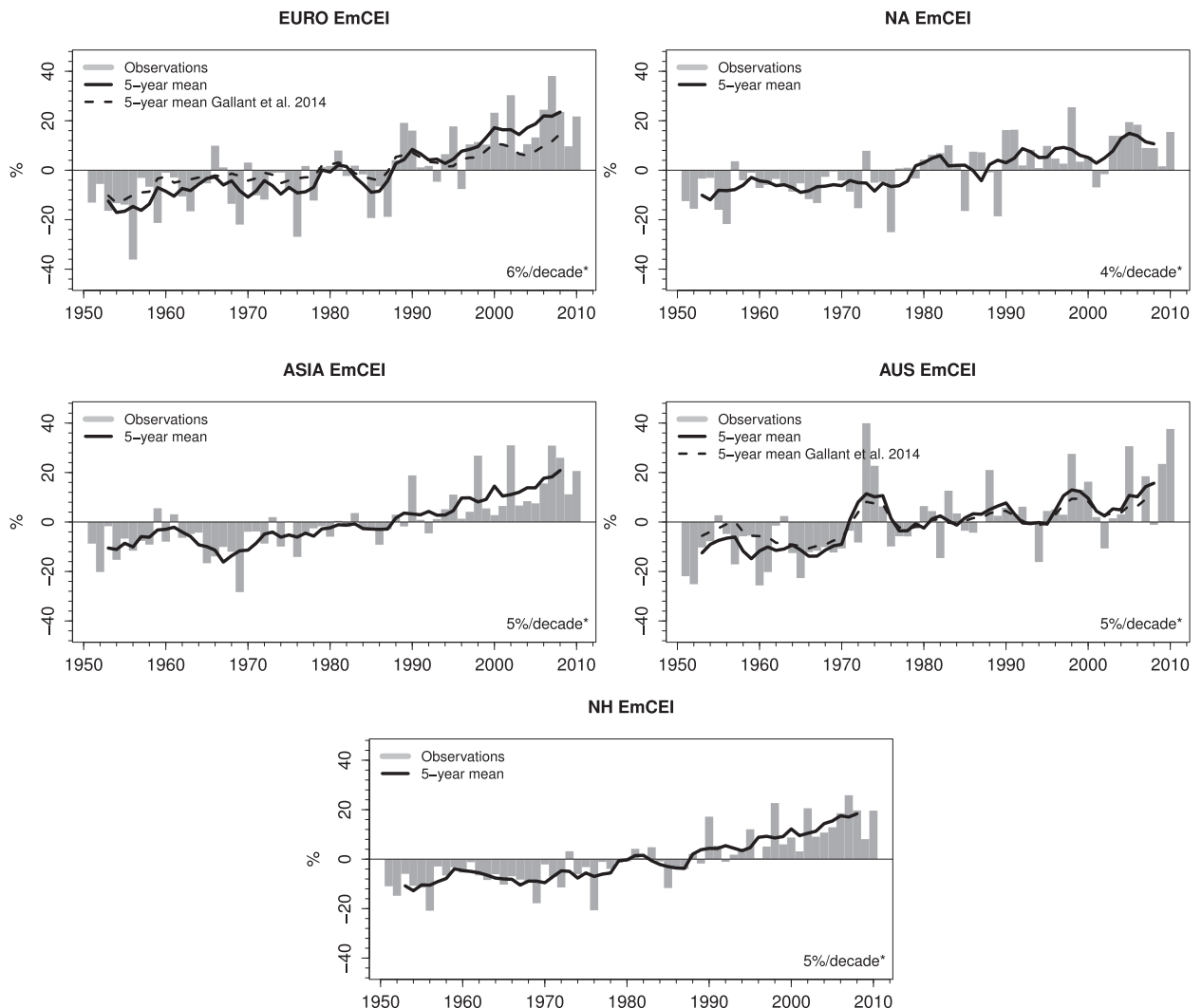
FIG. 8. The EmCEI for all regions. Trends (% decade^{-1}) were calculated using the nonparametric Theil–Sen slope estimator. An asterisk indicates statistical significance at the 5% level using the Mann–Kendall trend test.

large-scale increase in the areas experiencing extreme precipitation amounts, an extreme proportion of precipitation from heavy rainfall events, and an extreme number of wet days. There is less variability in the three precipitation components than for any region individually, as interannual variability is reduced when considering larger areas.

f. Relationship between components and combined index

For consistency with previous studies, we show the average of all components, corresponding to the EmCEI. For all regions, an increase in the EmCEI between 4% and 6% decade^{-1} is found (Fig. 8). It represents the "average area" experiencing extreme conditions in the five components. Positive values indicate that more areas

were experiencing warm/wet extremes than cold/dry extremes, and vice versa. As this is an average over five indicators, it cannot represent trends in any one component specifically, but it provides an overview of all components together. For example, increasing trends in the EmCEI are found in all regions even though trends in the precipitation components are found only for Europe, North America, and the Northern Hemisphere. The combined index should thus be viewed as a summary of the individual components, and not as a standalone indicator.

One interesting aspect of the combined index is whether it has an enhanced long-term-trend-to-interannual noise ratio compared with any single component. This is found to be true for all regions except Asia and the Northern Hemisphere. In Asia (and the Northern Hemisphere), the trend in the minimum temperature component is so

TABLE 5. Spearman correlation coefficients between each component (C1–C5) and area-mean temperature anomalies (T) and area-mean precipitation total (P) from CRUTEM4 (Jones et al. 2012) and GPCC (Schneider et al. 2011, 2014; Becker et al. 2013), respectively. The GPCC dataset has been regridded to HadEX2 resolution and masked to the coverage shown in Fig. 1 for all regions, while in the case of CRUTEM4 the mask (Fig. 1) was regridded to the resolution of CRUTEM4. The data have been detrended using the Theil–Sen trend estimate prior to the calculation of the correlation coefficients. The low-pass correlation coefficients have been calculated using 5-yr running means.

Region	C1–T	C2–T	C3–P	C4–P	C4–T	C5–P	EmCEI–T	EmCEI–P
Europe	0.80	0.75	0.83	−0.01	0.15	0.76	0.64	0.48
Europe low pass	0.88	0.78	0.74	0.24	0.66	0.60	0.71	0.49
NA	0.82	0.74	0.85	0.28	0.05	0.81	0.52	0.49
NA low pass	0.85	0.83	0.94	−0.02	0.07	0.95	0.38	0.29
Asia	0.79	0.66	0.83	0.61	0.13	0.57	0.70	0.61
Asia low pass	0.90	0.84	0.77	0.59	0.58	0.27	0.87	0.63
Australia	0.67	0.64	0.82	0.66	−0.28	0.80	0.25	0.55
Australia low pass	0.58	0.54	0.82	0.70	−0.49	0.79	0.13	0.66
NH	0.88	0.78	0.89	0.35	0.36	0.67	0.75	0.54
NH low pass	0.95	0.92	0.81	0.09	0.63	0.59	0.89	0.24

strong that it has the strongest trend-to-noise ratio (not shown). In North America and Australia at the interannual time scale, warm extremes are often associated with dry extremes and cold extremes with wet extremes (not shown). Hence, the warm and wet combination in the CEI reduces the interannual variability and allows any long-term change to be investigated. For Europe, the maximum temperature component and the total precipitation and wet/dry day components are uncorrelated. A weak positive correlation between both temperature components and the heavy precipitation component is found (0.28 and 0.31, respectively). In this case, the enhanced trend-to-noise ratio is simply due to the interannual variability being reduced from averaging in the presence of large trends in all components. This signal enhancement is likely to be relevant for detection and attribution studies.

It should be noted that the use of a combined index is controversial, as it may lead to difficulties with interpretation and the choice of indicators is somewhat subjective. The current set of components was designed to include two temperature and two precipitation extremes components, as well as a long-term drought component, which has been replaced by a long-term precipitation component in this study. We emphasize that the combined index is useful for summary purposes but should not be used without consideration of the individual components.

4. Discussion

The temperature components are highly correlated with interannual (detrended) variations of mean temperature over the same region, with correlation coefficients exceeding 0.7 in most regions (Table 5). This suggests that the increases in area with much-above-normal number of warm days and nights are related to a shift in the mean of the temperature distribution toward warmer temperatures for all regions. The fact that percentage area with above-average warm days is increasing but the percentage area of cold extremes is decreasing suggests that a change of variance alone cannot be the cause of the increases in the area affected by hot extremes. However, our results do not exclude changes in other moments of the distribution. This supports the use of the modified version of the original CEI introduced by Gallant and Karoly (2010), in which the lower-tail extremes are subtracted from the upper-tail extremes rather than adding both tails as in Karl et al. (1996).

The total rainfall component is also highly correlated to interannual variations of mean precipitation, exceeding 0.8 for all regions. The proportion of heavy rainfall component is strongly correlated to total precipitation in Asia and Australia, but not in the other regions. This is not particularly surprising, as interannual variations of the proportion of heavy precipitation would not necessarily be expected to be closely related to mean precipitation. However, there appears to be a possible link between mean temperature and the heavy precipitation component in some parts of the Northern Hemisphere, particularly Europe. To analyze this further, seasonal precipitation indices would be required; however, these are currently not available. The relationship between the heavy rainfall component and mean temperature over Australia is of the opposite sign, which is again likely due to the influence of ENSO over this region. The wet- and dry-day component is relatively highly correlated with total precipitation changes over most regions, except Asia. The correlation coefficients tend to be stronger when calculated on data that have not been detrended (not shown). These correlations suggest that the observed increases in the area affected by hot and wet extremes and decreases in cold and dry extremes may be closely

related to changes in the mean of the temperature and precipitation distributions, with the exception of the heavy rainfall component.

The combination of warm and wet, and cool and dry extremes used here is optimal for large areas. Recombining warm and dry and cool and wet extremes would be easily achieved, and may be useful over smaller regions where increases in dry extremes are associated with the long-term warming trend, such as in subtropical regions. This was done in Gallant and Karoly (2010) for southwestern and southeastern Australia. However, using smaller regions and grouping regions with similar climates would require higher-resolution data. It would also be useful in future analyses to investigate the EmCEI at the seasonal scale to determine whether the changes identified here occur predominantly for warm or cool season extremes. However, this is currently not possible as some ETCCDI indices are not available with monthly or seasonal frequency.

5. Conclusions

A new method of calculating the areal extent of five types of temperature and precipitation extremes based on standard extreme indices is introduced in this study. These five components are combined to form the climate extremes index. Although climate extremes indices have been presented before, this new index provides a computationally efficient method to monitor changes in the spatial extent of temperature and precipitation extremes combined. It can be updated in near–real time as more data become available. Spatial consistency in extremes is often overlooked, as most studies focus on trends in area averages or trend maps. Analysis of changes in extremes from an areal extent perspective, however, can be useful to complement our understanding of changes in temperature and precipitation extremes. For example, Fischer et al. (2013) have shown that there is reasonable agreement in projected changes in temperature and precipitation extremes for large ensembles of model simulations (both for a single model and multiple models) when looking at the overall fraction of area experiencing a certain magnitude of change, despite disagreement at the gridbox level resulting from internal variability. Here, the four continental-scale regions of Europe, North America, Asia, and Australia are analyzed. This study presents the first CEI results for large parts of Asia as well as the first study including daily-scale temperature extremes for North America. Furthermore, it is also the first time that a variant of the CEI has been computed at the hemispheric scale for the Northern Hemisphere.

The results show clear increases in the spatial prevalence of the extreme number of warm days and nights, and decreases in the spatial prevalence of the extreme number of cool days and nights for all regions, with the exception of North America, where no statistically significant trends in the area experiencing maximum temperature extremes are observed. Concurrently, the spatial extent of much-above-normal annual precipitation and the much-above-normal contribution from heavy rain days has also increased over the Northern Hemisphere, particularly over Europe and North America. Over Australia, the changes in the precipitation components are small and are dominated by large decadal variability. The combined index shows increases between 4% and 6% for all regions, indicating a large-scale increase in area experiencing warm and in some cases wet extremes across both hemispheres. Our findings are largely consistent with the results of GKG2014 and complement their results, with the exception of the total and heavy precipitation components over Europe. However, we think these differences are primarily due to differences in data source and resolution. In the case of the total precipitation component, a change from a Palmer drought severity index–based component to a solely precipitation-based component is also likely to contribute to these differences.

These results document a rapid increase in the area affected by much-above-normal warm extremes and, in some areas of the Northern Hemisphere, wet extremes and decreases in the area affected by cool extremes. While these types of extremes may be considered moderate, a shift toward more frequent warm and wet extremes and less frequent cool extremes occurring over increasingly large areas can put agricultural and natural systems under stress. There is thus a need to continue to monitor and understand how the area affected by these extremes changes, which can be achieved using the methodology presented here. However, data availability remains a major obstacle to this, particularly in the Southern Hemisphere. A model evaluation and attribution study of observed variability and trends using this framework is currently being undertaken to investigate possible causes of the observed changes described here.

REFERENCES

Alexander, L. V., and Coauthors, 2006: Global observed changes in daily climate extremes of temperature and precipitation. *J. Geophys. Res.*, **111**, D05109, doi:10.1029/2005JD006290.

Becker, A., P. Finger, A. Meyer-Christoffer, B. Rudolf, K. Schamm, U. Schneider, and M. Ziese, 2013: A description of the global land-surface precipitation data products of the Global Precipitation Climatology Centre with sample applications including centennial (trend) analysis from 1901–present. *Earth Syst. Sci. Data*, **5**, 71–99, doi:10.5194/essd-5-71-2013.

Bronaugh, D., and A. Werner, 2013: Zhang + Yue-Pilon trends package. R Package Version 0.10-1. [Available online at https://cran.r-project.org/web/packages/zyp/index.html.]

Donat, M. G., L. V. Alexander, H. Yang, I. Durre, R. Vose, and J. Caesar, 2013a: Global land-based datasets for monitoring climatic extremes. *Bull. Amer. Meteor. Soc.*, **94**, 997–1006, doi:10.1175/BAMS-D-12-00109.1.

——, and Coauthors, 2013b: Updated analyses of temperature and precipitation extreme indices since the beginning of the twentieth century: The HadEX2 dataset. *J. Geophys. Res.*, **118**, 2098–2118, doi:10.1002/jgrd.50150.

Fischer, E. M., U. Beyerle, and R. Knutti, 2013: Robust spatially aggregated projections of climate extremes. *Nat. Climate Change*, **3**, 1033–1038, doi:10.1038/nclimate2051.

Gallant, A. J. E., and D. J. Karoly, 2010: A combined climate extremes index for the Australian region. *J. Climate*, **23**, 6153–6165, doi:10.1175/2010JCLI3791.1.

——, ——, and K. L. Gleason, 2014: Consistent trends in a modified climate extremes index in the United States, Europe, and Australia. *J. Climate*, **27**, 1379–1394, doi:10.1175/JCLI-D-12-00783.1.

Gleason, K. L., J. H. Lawrimore, D. H. Levinson, T. R. Karl, and D. J. Karoly, 2008: A revised U.S. climate extremes index. *J. Climate*, **21**, 2124–2137, doi:10.1175/2007JCLI1883.1.

Groisman, P. Ya., R. W. Knight, D. R. Easterling, T. R. Karl, G. C. Hegerl, and V. N. Razuvaev, 2005: Trends in intense precipitation in the climate record. *J. Climate*, **18**, 1326–1350, doi:10.1175/JCLI3339.1.

Gruza, C., E. Rankova, V. Razuvaev, and O. Bulygina, 1999: Indicators of climate change for the Russian Federation. *Climatic Change*, **42**, 219–242, doi:10.1023/A:1005480719118.

Jones, P. D., D. H. Lister, T. J. Osborn, C. Harpham, M. Salmon, and C. P. Morice, 2012: Hemispheric and large-scale land-surface air temperature variations: An extensive revision and an update to 2010. *J. Geophys. Res.*, **117**, D05127, doi:10.1029/2011JD017139.

Jones, P. W., 1999: First- and second-order conservative remapping schemes for grids in spherical coordinates. *Mon. Wea. Rev.*, **127**, 2204–2210, doi:10.1175/1520-0493(1999)127<2204:FASOCR>2.0.CO;2.

Karl, T. R., R. W. Knight, D. R. Easterling, and R. G. Quayle, 1996: Indices of climate change for the United States. *Bull. Amer. Meteor. Soc.*, **77**, 279–292, doi:10.1175/1520-0477(1996)077<0279:IOCCFT>2.0.CO;2.

Kendall, M. G., 1975: *Rank Correlation Methods.* 4th ed. Charles Griffin, 202 pp.

Klein Tank, A. M. G., and G. P. Können, 2003: Trends in indices of daily temperature and precipitation extremes in Europe, 1946–99. *J. Climate*, **16**, 3665–3680, doi:10.1175/1520-0442(2003)016<3665:TIIODT>2.0.CO;2.

——, and Coauthors, 2006: Changes in daily temperature and precipitation extremes in central and south Asia. *J. Geophys. Res.*, **111**, D16105, doi:10.1029/2005JD006316.

Menne, M. J., I. Durre, R. S. Vose, B. E. Gleason, and T. G. Houston, 2012: An overview of the Global Historical Climatology Network-Daily database. *J. Atmos. Oceanic Technol.*, **29**, 897–910, doi:10.1175/JTECH-D-11-00103.1.

Moberg, A., and Coauthors, 2006: Indices for daily temperature and precipitation extremes in Europe analyzed for the period 1901–2000. *J. Geophys. Res.*, **111**, D22106, doi:10.1029/2006JD007103.

Nicholls, N., W. Drosdowsky, and B. Lavery, 1997: Australian rainfall variability and change. *Weather*, **52**, 66–72, doi:10.1002/j.1477-8696.1997.tb06274.x.

Risbey, J. S., M. J. Pook, P. C. McIntosh, M. C. Wheeler, and H. H. Hendon, 2009: On the remote drivers of rainfall variability in Australia. *Mon. Wea. Rev.*, **137**, 3233–3253, doi:10.1175/2009MWR2861.1.

Schneider, U., A. Becker, P. Finger, A. Meyer-Christoffer, B. Rudolf, and M. Ziese, 2011: GPCC full data reanalysis version 6.0 at 2.5°: Monthly land-surface precipitation from rain-gauges built on GTS-based and historic data. Deutscher Wetterdienst, accessed 31 March 2014, doi:10.5676/DWD_GPCC/FD_M_V6_250.

——, ——, ——, ——, M. Ziese, and B. Rudolf, 2014: GPCC's new land surface precipitation climatology based on quality-controlled in situ data and its role in quantifying the global water cycle. *Theor. Appl. Climatol.*, **115**, 15–40, doi:10.1007/s00704-013-0860-x.

Sen, P. K., 1968: Estimates of the regression coefficient based on Kendall's tau. *J. Amer. Stat. Assoc.*, **63**, 1379–1389, doi:10.1080/01621459.1968.10480934.

Seneviratne, S. I., and Coauthors, 2012: Changes in climate extremes and their impacts on the natural physical environment. *Managing the Risks of Extreme Events and Disasters to Advance Climate Change Adaptation*, C. B. Field et al., Eds., Cambridge University Press, 109–230.

Sheffield, J., E. F. Wood, and M. L. Roderick, 2012: Little change in global drought over the past 60 years. *Nature*, **491**, 435–438, doi:10.1038/nature11575.

Wang, X. L., and V. R. Swail, 2001: Changes of extreme wave heights in Northern Hemisphere oceans and related atmospheric circulation regimes. *J. Climate*, **14**, 2204–2221, doi:10.1175/1520-0442(2001)014<2204:COEWHI>2.0.CO;2.

You, Q., and Coauthors, 2011: Changes in daily climate extremes in China and their connection to the large scale atmospheric circulation during 1961–2003. *Climate Dyn.*, **36**, 2399–2417, doi:10.1007/s00382-009-0735-0.

Zhang, X., and F. W. Zwiers, 2004: Comment on "Applicability of prewhitening to eliminate the influence of serial correlation on the Mann-Kendall test" by Sheng Yue and Chun Yuan Wang. *Water Resour. Res.*, **40**, W03805, doi:10.1029/2003WR002073.

——, L. A. Vincent, W. D. Hogg, and A. Niitsoo, 2000: Temperature and precipitation trends in Canada during the 20th century. *Atmos.–Ocean*, **38**, 395–429, doi:10.1080/07055900.2000.9649654.

——, L. Alexander, G. C. Hegerl, P. Jones, A. K. Tank, T. C. Peterson, B. Trewin, and F. W. Zwiers, 2011: Indices for monitoring changes in extremes based on daily temperature and precipitation data. *Wiley Interdiscip. Rev.: Climate Change*, **2**, 851–870, doi:10.1002/wcc.147.

Zhou, Y., and G. Ren, 2011: Change in extreme temperature event frequency over mainland China, 1961–2008. *Climate Res.*, **50**, 125–139, doi:10.3354/cr01053.